# Human aldolase A natural mutants: relationship between flexibility of the C-terminal region and enzyme function

Gabriella ESPOSITO*†[1], Luigi VITAGLIANO‡[1], Paola COSTANZO*†, Loredana BORRELLI*†, Rita BARONE§, Lorenzo PAVONE§, Paola IZZO*†, Adriana ZAGARI†‡‖ and Francesco SALVATORE*†[2]

*Dipartimento di Biochimica e Biotecnologie Mediche, Università di Napoli "Federico II", Via S. Pansini 5, I-80131 Napoli, Italy, †CEINGE–Biotecnologie Avanzate, Università di Napoli "Federico II", Via S. Pansini 5, I-80131 Napoli, Italy, ‡Istituto di Biostrutture e Bioimmagini, CNR, Via Mezzocannone 6, I-80134 Napoli, Italy, §Dipartimento di Pediatria, Policlinico, Università di Catania, Via S. Sofia 78, I-95123 Catania, Italy, and ‖Dipartimento di Chimica Biologica, Università di Napoli "Federico II", Via Mezzocannone 6, I-80134 Napoli, Italy

We have identified a new mutation in the FBP (fructose 1,6-bisphosphate) aldolase A gene in a child with suspected haemolytic anaemia associated with myopathic symptoms at birth and with a subsequent diagnosis of arthrogryposis multiplex congenita and pituitary ectopia. Sequence analysis of the whole gene, also performed on the patient's full-length cDNA, revealed only a $Gly^{346} \rightarrow Ser$ substitution in the heterozygous state. We expressed in a bacterial system the new aldolase A $Gly^{346} \rightarrow Ser$ mutant, and the $Glu^{206} \rightarrow Lys$ mutant identified by others, in a patient with an aldolase A deficit. Analysis of their functional profiles showed that the $Gly^{346} \rightarrow Ser$ mutant had the same $K_m$ as the wild-type enzyme, but a 4-fold lower $k_{cat}$. The $Glu^{206} \rightarrow Lys$ mutant had a $K_m$ approx. 2-fold higher than that of both the $Gly^{346} \rightarrow Ser$ mutant and the wild-type enzyme, and a $k_{cat}$ value 40 % less than the wild-type. The $Gly^{346} \rightarrow Ser$ and wild-type enzymes had the same $T_m$ (melting temperature), which was approx. 6–7 °C higher than that of the $Glu^{206} \rightarrow Lys$ enzyme. An extensive molecular graphic analysis of the mutated enzymes, using human and rabbit aldolase A crystallographic structures, suggests that the $Glu^{206} \rightarrow Lys$ mutation destabilizes the aldolase A tetramer at the subunit interface, and highlights the fact that the glycine-to-serine substitution at position 346 limits the flexibility of the C-terminal region. These results also provide the first evidence that $Gly^{346}$ is crucial for the correct conformation and function of aldolase A, because it governs the entry/release of the substrates into/from the enzyme cleft, and/or allows important C-terminal residues to approach the active site.

Key words: aldolase A, aldolase A mutant expression, aldolase A gene mutation, fructose 1,6-bisphosphate, molecular modelling.

## INTRODUCTION

Vertebrate fructose 1,6-bisphosphate (FBP) aldolase (EC 4.1.2.13), which exists in three isoforms, namely aldolase A, B and C, catalyses the reversible conversion of FBP and fructose 1-phosphate into two triose molecules in the glycolytic, gluconeogenic and fructose metabolic pathways [1]. Aldolase B is mainly expressed in the liver, kidney and small intestine, where it serves a role in exogenous fructose utilization. Aldolase A is a ubiquitous and constitutively expressed housekeeping enzyme that drives the glycolytic metabolic pathway in most mammalian cells. Aldolase C is expressed predominantly in the brain [1]. Aldolase B deficiency has been widely described in humans, because it causes HFI [hereditary fructose intolerance; OMIM (Online Mendelian Inheritance in Man) #229600], which is an autosomal recessive disease that may induce severe liver damage, leading, in extreme cases, to death if fructose is not eliminated from the diet [2]. To date, nearly 25 HFI-related aldolase B mutants have been isolated [3–7]. In contrast, cases of aldolase A deficiency, which has been associated with non-spherocytic haemolytic anaemia (OMIM #103850), are much rarer [8–12].

Aldolase A deficiency is an autosomal recessive trait, with alterations in the aldolase A gene leading to amino acid substitutions ($Asn^{128} \rightarrow Gly$ and $Glu^{206} \rightarrow Lys$) in two of the few cases already described [10–12]. It is conceivable that, given the essential function of this enzyme in almost all human tissues, human embryos affected by severe aldolase A mutations do not survive. Biochemical and thermodynamic data are available for the $Asn^{128} \rightarrow Gly$ mutant [10], whereas the $Glu^{206} \rightarrow Lys$ mutant has never been characterized. Here, we report a novel defect in the aldolase A gene, i.e. a natural mutation at amino acid residue 346 ($Gly \rightarrow Ser$), which appears to be a bending site that is important for the functioning of the enzyme. We also report the expression and characterization of the $Gly^{346} \rightarrow Ser$ and $Glu^{206} \rightarrow Lys$ natural mutant enzymes.

## EXPERIMENTAL

### Materials

Restriction endonucleases were from New England Biolabs. *Taq* polymerase, T4 DNA ligase, IPTG (isopropyl $\beta$-D-thiogalactoside), ampicillin, PMSF and GDH/TIM ($\alpha$-glycerol phosphate dehydrogenase/triose phosphate isomerase) were from Roche Molecular Biochemicals. Imidazole, FBP and NADH were from Sigma–Aldrich. The pET-16b vector and the *Escherichia coli* strain BL21(DE3) were purchased from Novagen.

### The patient

The proband is a 7-year-old Italian boy examined at the age of 3 months [13], in whom aldolase A deficiency was initially suspected because of muscle weakness and presumed haemolytic anaemia. Both parents are healthy and non-consanguineous.

Abbreviations used: ARMS, amplification refractory mutation system; DHAP, dihydroxyacetone phosphate; FBP, fructose 1,6-bisphosphate; GDH/TIM, $\alpha$-glycerol phosphate dehydrogenase/triose phosphate isomerase; HFI, hereditary fructose intolerance; OMIM, Online Mendelian Inheritance in Man; PDB, Protein Data Bank; RT, reverse transcriptase; $T_m$, melting temperature.

[1] These authors contributed equally to this work.

[2] To whom correspondence should be addressed, at the Dipartimento di Biochimica e Biotecnologie Mediche (e-mail salvator@unina.it).

**Table 1 Primers used for ARMS analysis**

ARMS 346 Norm and ARMS 346 Mut are allele-specific forward primers; 'Common' is a reverse primer, within the aldolase A intron 9; and Forward control and Reverse control are primers within the $\beta$-globin gene.

| Primer | Sequence | Concentration ($\mu$M) |
|---|---|---|
| ARMS 346 Norm | 5′-AGGAAAGTACACTCCGTGCG-3′ | 0.5 |
| ARMS 346 Mut | 5′-AGGAAAGTACACTCCGTGCA-3′ | 0.5 |
| Common | 5′-CACTTGGCAGGAACACTTGT-3′ | 0.15 |
| Forward control | 5′-CCTTGGACCCAGAGGTTCTT-3′ | 0.1 |
| Reverse control | 5′-AATCATTCGTCTGTTTCCCT-3′ | 0.1 |

### Genetic analysis

Genomic DNA was purified from peripheral blood leucocytes by the NaCl extraction method [14]. The whole aldolase A-coding region, the splice junctions and the promoter regions were amplified by PCR using appropriate primer pairs (GenBank® #NT_010604). The amplified DNA fragments were automatically sequenced using fluorescence-based methods (Big Dye™ Terminator, ABI Prism 377 DNA Sequencer; PE Applied Biosystems, Foster City, CA, U.S.A.) with the ABI-Prism 377 Applied Biosystems Genetic analyser (PE Applied Biosystems). The sequence data were analysed by a visual check for heterozygous mutations. We used the ARMS (amplification refractory mutation system) analysis [15] to examine Mendelian inheritance of the $Gly^{346} \rightarrow Ser$ mutation in the proband's family. DNA samples were amplified in two reactions containing 0.2 $\mu$g of genomic DNA and 1 unit *Taq* polymerase (PerkinElmer/Cetus). After an initial denaturing step of 1 min at 94 °C, samples were amplified for 32 cycles at 94 °C for 20 s, 55 °C for 20 s and 72 °C for 30 s. At a final volume of 50 $\mu$l, each reaction mixture contained 200 $\mu$M of each dNTP, 50 mM KCl, 10 mM Tris/HCl, pH 8.8, 2.5 mM $MgCl_2$, 0.01 % (w/v) gelatin, the appropriate forward ARMS primer, a common reverse primer and an additional primer pair that amplified a $\beta$-globin gene fragment, which is an internal control of amplification conditions (Table 1). The results were analysed on a 2 % (w/v) agarose gel.

Total RNA extracted from the patient's peripheral blood by the QIAamp RNA Blood Mini Kit (Qiagen Inc.) was first analysed by Northern blotting using the aldolase A cDNA as a probe, and then subjected to RT (reverse transcriptase)-PCR using specific primers (plus and minus primer; see below) and the SuperScript™ III One-Step RT-PCR System (Invitrogen, Milan, Italy). The amplified fragment, corresponding to the patient's aldolase A cDNA, was subjected to automated sequencing.

### Construction and expression of wild-type and mutant aldolase A

The full-length wild-type human aldolase A cDNA [16] was amplified with the forward primer containing a *Nde*I site (shown underlined) at the 5′-end (plus primer: 5′-GGAATTCCATATG-CCCTACCAATATCCAGC-3′), and the reverse primer containing the aldolase A termination codon (UAA) followed by a *Bam*HI site (also shown underlined) (minus primer: 5′-GGAATTCG-GATCCTTAATAGGCGTGGTTAG-3). The cDNA sequence was verified by automated sequencing. The amplified cDNA was cloned into the *Nde*I and *Bam*HI sites of the bacterial expression vector pET-16b, downstream of a His-tag coding sequence. To select recombinant clones, *E. coli* XL1-Blu host cells were transformed with the vector containing the target gene. Recombinant plasmid (pET-16b/cDNA) was purified over a Qiagen column (Qiagen).

The QuickChange™ site-directed mutagenesis kit (Stratagene) was used to introduce mutations into the pET-16b/cDNA construct. Mutagenesis reactions were carried out with a PerkinElmer 9600 thermal cycler. To change the normal $Glu^{206}$ into a lysine residue, primers 5′-CAGTATGTGACCAAGAAGGTGCTGG-3′ (sense) and 5′-CCAGCACCTTCTTGGTCACATACTG-3′ (antisense) were synthesized. To change $Gly^{346}$ into a serine, the sense primer was 5′-CACTCCGAGCAGTCAGGCTGG-3′ and the antisense primer was 5′-CCAGCCTGACTGCTCGGAGTG-3′. The parental methylated DNA was digested with *Dpn*I, and the newly synthesized DNA was used to transform the *E. coli* XL1-Blu competent cells, according to the manufacturer's instructions. Recombinant mutated plasmids were purified over Qiagen columns, and their full sequences were verified by automated sequencing. Recombinant aldolase A proteins were expressed in the *E. coli* B strain BL21(DE3). All the wild-type, $Glu^{206} \rightarrow Lys$ and $Gly^{346} \rightarrow Ser$ proteins were recovered in soluble form in bacteria grown at 37 °C. Recombinant enzymes were purified on $Ni^{2+}$/nitrilotriacetate resin (Qiagen), as described elsewhere [7,17]. Fractions containing the bulk of the enzyme were pooled, dialysed against 20 mM Tris/HCl, pH 7.5/50 % (v/v) glycerol, and stored at − 20 °C. All purification steps were performed at 4 °C. The purity degree of each recombinant enzyme was analysed by SDS/PAGE [10 % (w/v) gel].

### Molecular mass determination, denaturation profile analysis and CD spectra

Enzyme molecular masses were determined at 25 °C by co-fractionation (on FPLC) of the purified proteins with $\beta$-amylase (200 kDa), chicken ovalbumin (44 kDa) and carbonic anhydrase (29 kDa) on a 50 cm × 1.6 cm Sephadex G-200 column (Amersham Pharmacia Biotech.) in 20 mM Tris/HCl, pH 7.4/20 % (v/v) glycerol, with a flow rate of 0.2 ml/min. CD spectra were recorded at 20 °C using a Jasco J-810 spectropolarimeter equipped with a cuvette with a 0.1 cm path length. The molar ellipticity ($[\theta]$ in $deg \cdot cm^2 \cdot dmol^{-1}$) was calculated from the equation $[\theta] = [\theta]_{obs} \cdot mrw/10 \cdot l \cdot C$, where $[\theta]_{obs}$ is the measured ellipticity in degrees, mrw is the mean residue molecular weight, l is the optical path length of the cuvette in cm, and C is the protein concentration expressed in $g \cdot l^{-1}$. Spectra were recorded from 190–250 nm, with a scanning speed of 20 nm/min. Thermal denaturation data on the recombinant proteins were collected using a scan rate of 1 °C/min in the range 20–80 °C. CD experiments were performed with a protein concentration of 1 mg/ml in 20 mM Tris/HCl, pH 7.2.

### Aldolase A activity assays and kinetic studies

The substrate cleavage rate was determined spectrophotometrically by measuring NADH oxidation at 340 nm in a coupled assay using GDH/TIM, with FBP as the substrate [18]. Assays were conducted at 30 °C, as described previously [7]. One unit of activity corresponds to the cleavage of 1 $\mu$mol of hexose substrate/min. Specific activity was obtained by normalizing for mg of protein. For each recombinant enzyme, we ran three assays with at least two different enzyme preparations, and evaluated the $K_m$ and $k_{cat}$ values from double-reciprocal plots using a least-squares method. The kinetic data that were fitted directly to the Michaelis–Menten equation gave the same $k_{cat}$ and $K_m$ values calculated from the double-reciprocal plot.

### Molecular graphics analyses

The alterations induced by mutations in the aldolase A structure were evaluated by molecular graphics using the crystallographic structures of human and rabbit aldolase A reported in the PDB

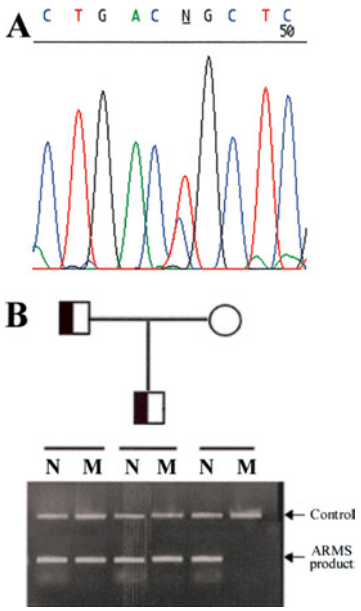


**Figure 1 Identification of the Gly$^{346}$ → Ser mutation in the aldolase A gene**

(**A**) Sequencing of the mutated region (antisense strand). 'N' indicates the co-elution of the normal C and the mutated T nucleotides (G and A respectively on the sense strand), as expected for a heterozygous subject. (**B**) ARMS analysis confirms the Mendelian transmission of the mutation in the family (see the text for further details). The lanes of the gel correspond to the subjects shown in the family's pedigree. The pattern of a normal subject is represented in the lane corresponding to the proband's mother. N, normal primer; M, mutated primer.

(Protein Data Bank) [19]. In particular, the effect of the mutation of Glu$^{206}$ was analysed considering its interactions in all aldolase A structures (PDB codes 1ALD, 1ADO, 2ALD, 4ALD, 6ALD, 1J4E, 1EX5, 1EWG and 1EWD) [20–25]. Because the C-terminal region is often disordered in the aldolase A structure, we analysed the effects of the Gly$^{346}$ → Ser mutation considering only the complexes of human aldolase A (4ALD) with FBP [22] and of rabbit aldolase A with DHAP (dihydroxyacetone phosphate; 1ADO) [21]. These analyses were performed using the Insight II, PROMOTIF [26], O [27] and PROCHECK [28] programs. Figures 3 and 4 were generated with MolScript [29] and Raster3D [30].

## RESULTS

### Genetic analysis

The proband's aldolase A gene was analysed by direct sequencing of the whole coding region and of the splice junctions. We found only one alteration at the heterozygous state in exon 9 with respect to the normal gene sequence, i.e. a G → A substitution at nt 17006 (GenBank® #NT_010604), which changes Gly$^{346}$ into a serine residue (Figure 1A). We confirmed the Mendelian transmission of the mutation in the family by ARMS, and established that the proband inherited the Gly$^{346}$ → Ser substitution from his father (Figure 1B). This novel aldolase A mutation was not found on 200 chromosomes from normal subjects, thereby excluding its presence in the normal population.

Total RNA from the patient, analysed by Northern blotting, showed a unique band for aldolase A, which was the same size as the wild-type mRNA (results not shown). Furthermore, RT-PCR gave a single amplification product corresponding to the full-length aldolase A cDNA. Sequencing of this fragment confirmed the presence of the Gly$^{346}$ → Ser mutation at the heterozygous state in the patient. No other mutations were detected in the patient's aldolase A mRNA.

### Expression and characterization of recombinant aldolase A proteins

We expressed the wild-type aldolase A protein, the Glu$^{206}$ → Lys mutant and the new aldolase A Gly$^{346}$ → Ser mutant in *E. coli*. The recombinant His-tagged proteins were purified to > 95 % homogeneity by $Ni^{2+}$-affinity chromatography, as verified by SDS/PAGE (results not shown). The recombinant enzymes were expressed in bacteria grown at 37 °C, and recovered from the soluble fraction of the bacterial lysate. The purification rate was 10–12 mg/l of culture for all recombinant proteins. The molecular mass of the recombinant enzymes, determined by FPLC, was approx. 170 kDa (Figure 2A). The enzymes remained stable at 4 °C in 20 mM Tris/HCl, pH 7.4, for at least 2 weeks, and for at least 1 month at − 20 °C in 50 % (v/v) glycerol/20 mM Tris/HCl, pH 7.4. CD spectra of wild-type, Glu$^{206}$ → Lys and Gly$^{346}$ → Ser recombinant aldolases revealed nearly identical curves within experimental error, suggesting that the three enzymes share very similar secondary structures (Figure 2B), and therefore that the mutations did not cause major perturbations in the enzyme's secondary structure.

The analysis of the thermal stability (Table 2, first column, and Figure 2C) of these recombinant forms of aldolase A reveals that the $T_m$ (melting temperature) of the Gly$^{346}$ → Ser mutant (54.8 °C) is virtually identical with that of the wild-type enzyme (54.4 °C). On the other hand, the replacement of a glutamic acid in position 206 with a lysine significantly reduces the thermal stability of the enzyme ($T_m$ 48.0 °C).

Analysis of the kinetic properties of aldolase A recombinant forms (Table 2) demonstrates that the Glu$^{206}$ → Lys and Gly$^{346}$ → Ser proteins display a reduced activity towards FBP, the physiological substrate of the enzyme. In particular, the reduction in specific activity was greater in the case of the Gly$^{346}$ → Ser mutant than Glu$^{206}$ → Lys. Although the catalytic efficiency of the two mutants was reduced by the same extent (i.e. to at least one-third lower compared with the wild-type enzyme), the Glu$^{206}$ → Lys and Gly$^{346}$ → Ser proteins have different $k_{cat}$ and $K_m$ values. In the case of the Gly$^{346}$ → Ser mutant, the decreased $k_{cat}/K_m$ ratio is mostly due to the decreased $k_{cat}$ value, whereas in the case of Glu$^{206}$ → Lys, it is due mainly to the increase in $K_m$. The intracellular FBP concentration of approx. 14 $\mu$M [31], lower than the $K_m$ value of the recombinant wild-type enzyme, is not sufficient to saturate the Glu$^{206}$ → Lys mutant enzyme (see Table 2), which hence would be less active than normal *in vivo*. This observation explains, at the molecular level, the severe disease phenotype of haemolytic anaemia and myopathy in the patient carrying the Glu$^{206}$ → Lys mutation in the homozygous state [11].

### Molecular graphics analyses

Aldolase A is physiologically active as a tetramer composed of four monomers each characterized by an eight-membered $\alpha/\beta$-barrel structure. The N-terminal helix and the C-terminal region are located at opposite ends of the central cavity of the barrel structure. The Gly$^{346}$ residue, conserved among vertebrate aldolase A sequences, is located in the C-terminal region of the enzyme. In aldolase A, this region is particularly flexible, and is thus frequently disordered in the various reported three-dimensional structures of the enzyme. However, a reliable tracing of this region has been obtained for human aldolase A complexed with FBP [22] and for rabbit aldolase A complexed with the reaction product DHAP [21]. Interestingly, in the AldA–DHAP complex, the C-terminus assumes different conformations in the different chains

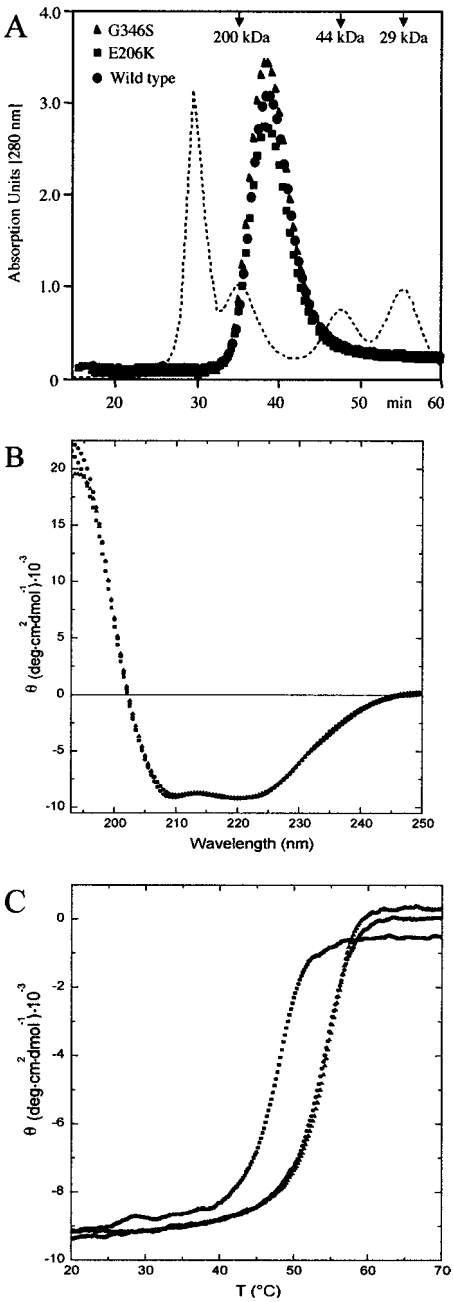


**Figure 2 Characterization of recombinant wild-type and mutant aldolases A**

(**A**) FPLC profiles of the wild-type and mutant aldolase A enzymes. The elution profiles indicate that all the recombinant enzymes have a molecular mass of approx. 170 kDa, as expected for the His-tagged homo-tetrameric form of aldolase A, purified under native conditions. The dotted line and arrows indicate the molecular masses of the protein standards used in calibration and apply to all three panels (see the Experimental section). (**B**) CD spectra of wild-type, $Gln^{206} \rightarrow Lys$ and $Gly^{346} \rightarrow Ser$ aldolase A recorded at a protein concentration of 0.4 mg/ml, at 20 °C as a function of wavelength. (**C**) Melting curves of wild-type, $Gln^{206} \rightarrow Lys$ and $Gly^{346} \rightarrow Ser$ aldolase A obtained by monitoring molar ellipticity at 222 nm.

of the tetramer, depending on the binding state of each subunit (Figure 3). In particular, when a DHAP molecule is bound to the subunit, the C-terminus folds over the surface of its own subunit [21]. On the other hand, in subunits with no DHAP bound to the active site, the C-terminus protrudes towards an intersubunit cleft of an adjacent tetramer, thereby leaving the active site fully exposed. In both the AldA–FBP and AldA–DHAP complexes, a serine residue could replace the glycine without any steric overlap, because residue 346 is exposed to the solvent. However, we underline that the main chain dihedral angles of $Gly^{346}$ in the AldA–FBP and AldA–DHAP complexes indicate that this residue assumes, in some cases, conformations that are usually unfavourable for non-glycine residues (Table 3).

The $Glu^{206}$ residue is located on the polar side of the amphipathic helix E (residues 197–219). This residue forms a strong intrasubunit salt bridge with $Arg^{258}$, which is the C-terminal residue of helix F (residues 244–258). Interaction between $Glu^{206}$ and $Arg^{258}$ may affect the tetramer stability, since the $Arg^{258}$ side chain is also involved in an intersubunit salt bridge with $Glu^{224}$ of an adjacent subunit (Figures 4A and B). The aldolase A tetramer is stabilized by four $Glu^{206}/Arg^{258}/Glu^{224}$ clusters of charged residues (Figure 4A). Interestingly, $Glu^{206}$, $Glu^{224}$ and $Arg^{258}$ are strictly conserved residues in vertebrate aldolase isoenzymes. These residues are also present in the sequences of insects and plants, such as *Drosophila melanogaster* and rice. The $Glu^{206}/Arg^{258}/Glu^{224}$ cluster (Figure 4B) has been detected in all vertebrate aldolase structures reported in the PDB, independently of the protein source, the binding state and the occurrence of mutations. In this framework, the replacement of $Glu^{206}$ with a positively charged lysine residue may severely perturb the structural integrity of the enzyme.

## DISCUSSION

Class I aldolases are important enzymes in glycolysis. Aldolase deficiencies may lead to severe genetic diseases. In particular, aldolase B deficiency in humans is linked to the widespread HFI, which affects 1 in 2000 newborns.

Mutations in the aldolase A gene are very rare *in vivo*. Thus far, only two naturally occurring mutations ($Asn^{128} \rightarrow Gly$ and $Glu^{206} \rightarrow Lys$) have been reported, both of which are associated with non-spherocytic haemolytic anaemia and myopathic symptoms [10,11]. Whereas a large body of biochemical and thermodynamic data is available for $Asn^{128} \rightarrow Gly$ [10], the $Glu^{206} \rightarrow Lys$ mutant has never been expressed and characterized.

Here, we report a novel naturally occurring mutation of aldolase A ($Gly^{346} \rightarrow Ser$), which has been found, in the heterozygous state, in an infant in whom an aldolase deficit was suspected, because of severe muscle weakness and presumed haemolytic anaemia. We have expressed and characterized the $Gly^{346} \rightarrow Ser$ and $Glu^{206} \rightarrow Lys$ mutants.

Analysis of the thermal stability of the two mutants indicates that the $Gly^{346} \rightarrow Ser$ enzyme is as stable as the wild-type, whereas replacement of $Glu^{206}$ with a lysine residue reduces the enzyme $T_m$ by 6.4 °C.

These results may be interpreted in view of the location of the mutated sites in the three-dimensional structure of the enzyme. Indeed, $Gly^{346}$ is located in the proximity of the flexible C-terminus, whereas $Glu^{206}$ is involved in strong electrostatic interactions at the subunit interfaces of the aldolase A tetramer. Remarkably, the destabilization of the $Glu^{206} \rightarrow Lys$ mutant is comparable with that reported for the disease-causing mutation, $Asn^{128} \rightarrow Gly$ [10].

From the biochemical viewpoint, both $Glu^{206} \rightarrow Lys$ and $Gly^{346} \rightarrow Ser$ mutants have a lower catalytic efficiency than wild-type aldolase A. However, a closer evaluation of the kinetic parameters revealed that the $k_{cat}/K_m$ ratio is reduced by different mechanisms in the two mutants. In the case of $Glu^{206} \rightarrow Lys$, both $K_m$ and $k_{cat}$ are significantly decreased, despite the distance [larger than 20 Å (1 Å ≡ 0.1 nm)] between the mutation site and the active site. This finding indicates that structural modifications

**Table 2 Functional enzymic parameters of the recombinant human aldolase A enzymes analysed**

Standard deviations of the mean values were derived from errors associated with multiple repeats of the experiment.

| Enzyme | $T_m$ (°C) | Specific activity ($\mu$mol · min$^{-1}$ · mg$^{-1}$) | $K_m$ ($\mu$M) | $k_{cat}$ (s$^{-1}$) | Catalytic efficiency $k_{cat}/K_m$ | Fold decrease |
|---|---|---|---|---|---|---|
| Wild-type | 54.4 | 22.3 ± 2.3 | 51.9 ± 6.5 | 16.7 ± 1.8 | 0.32 ± 0.07 | – |
| Mutant | | | | | | |
| Gly$^{346}$ → Ser | 54.8 | 6.1 ± 0.5 | 56.6 ± 5.2 | 4.7 ± 0.5 | 0.08 ± 0.01 | 4.0 |
| Gln$^{206}$ → Lys | 48.0 | 15.7 ± 3.4 | 105.0 ± 15.0 | 10.7 ± 1.7 | 0.10 ± 0.03 | 3.2 |

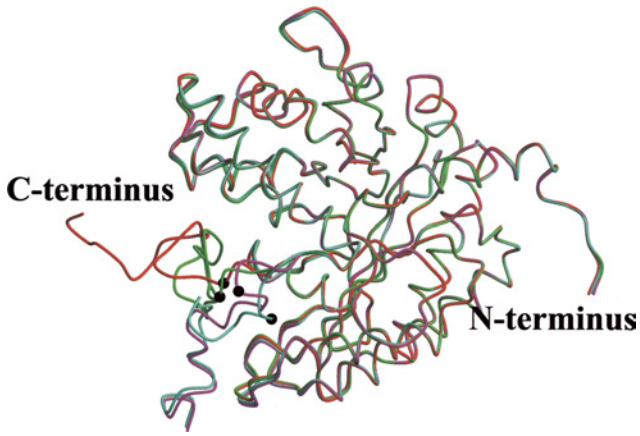


**Figure 3 Superimposition of the four subunits of aldolase A found in the complex with DHAP [21]**

Given the location of Gly$^{346}$ in each chain (black circles), this residue is clearly important for the flexibility of the C-terminal segment of the aldolase A protein.

**Table 3 Dihedral angles of Gly$^{346}$ in aldolase A structures**

PDB codes 4ALD and 1ADO refer, respectively, to the complexes of human aldolase A with FBP [22], and of rabbit aldolase A with DHAP [21].

| Structure | Subunit | $\varphi$ (°) | $\psi$ (°) |
|---|---|---|---|
| 1ADO | A | 68.6 | – 162.0 |
| 1ADO | B | 130.0 | – 31.5 |
| 1ADO | C | 53.7 | 28.3 |
| 1ADO | D | 119.9 | – 1.5 |
| 4ALD | A,B,C,D* | 113.1 | – 138.1 |

* The four chains of 4ALD present identical structures, since the asymmetric unit contains a single monomer.

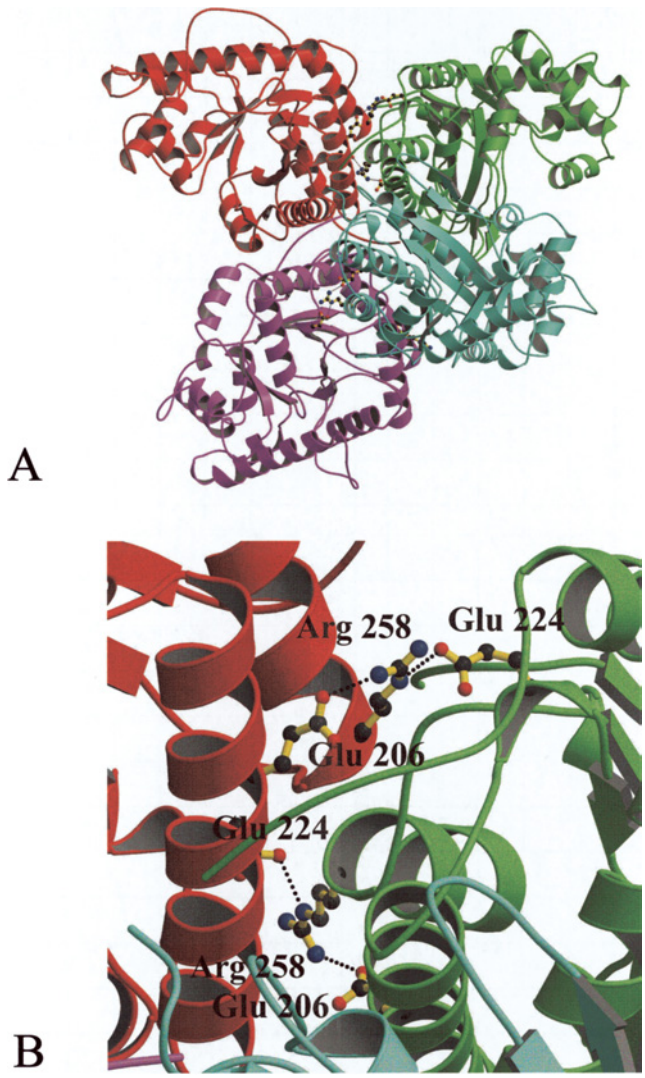


**Figure 4 Ion pairs involving residues Glu$^{206}$, Glu$^{224}$ and Arg$^{258}$ at monomer–monomer interfaces within the tetramer structure of aldolase A [21]**

(**A**) Location of the four clusters within the tetramer. (**B**) Close-up of two of the four charged clusters, showing in greater detail the positions of residues Arg$^{258}$, Glu$^{224}$, Glu$^{206}$ at the monomer–monomer interface.

at the intersubunit interface may be propagated towards the active-site regions via changes in the enzyme's tertiary and quaternary structures. A different picture emerges from the analysis of the kinetic parameters of the Gly$^{346}$ → Ser mutant, which has the same $K_m$ value as the wild-type enzyme and a significantly reduced $k_{cat}$. These observations are consistent with the structural data available for the aldolase A enzyme [21,25]. Indeed, it is not surprising that wild-type aldolase A and the Gly$^{346}$ → Ser mutant have a similar affinity for FBP since, as the structure of the AldA–FBP complex shows, neither Gly$^{346}$ nor the C-terminal region directly interacts with the substrate [22]. On the other hand, the lower $k_{cat}$ value of the Gly$^{346}$ → Ser mutant points to an alteration in the enzyme's catalytic properties as a consequence of a decreased flexibility of the C-terminus. The latter consideration is in line with the observations that: (i) the C-terminus adopts different conformations, depending on the binding mode of the reaction product (i.e. DHAP) to aldolase A [21]; and (ii) in

aldolase A structures, $Gly^{346}$ often adopts conformations that are energetically unfavourable for non-glycine residues, such as serine. Therefore the flexibility of the C-terminal region is important for the efficiency of aldolase A function.

In conclusion, our study was prompted by the discovery of a novel *in vivo* mutation of human aldolase A. Not only does our investigation lend additional support to the role of the flexible C-terminal region in the enzyme function [21,22], but it also provides a strong indication that $Gly^{346}$, a residue embodied within a hinge fragment at the C-terminus, is critical for the enzyme's activity.

We thank Dr Vincenzo Granata for help in recording CD spectra and Jean Ann Gilder for text editing. This work was supported by grants from the Ministero dell'Istruzione, dell'Università e della Ricerca (MIUR; Rome, Italy) and Consiglio Nazionale delle Ricerche (CNR) Target Project "Biotecnologie"; from Regione Campania "Ricerca Sanitaria Finalizzata" and Regione Molise (POP 1994–1999), Italy.

## REFERENCES

1 Salvatore, F., Izzo, P. and Paolella, G. (1986) Aldolase gene and protein families: structure, expression and pathophysiology. In Horizons in Biochemistry Biophysics (Blasi, F., ed.), vol. 8, pp. 611–665, John Wiley and Sons, Chichester
2 Steinmann, B., Gitzelmann, R. and Van den Berghe, G. (2001) Disorders of fructose metabolism. In The Metabolic and Molecular Bases of Inherited Disease, 7th edn (Scriver, C. S., Beaudet, A. L., Sly, W. S. and Valle, D., eds.), pp. 1489–1520, McGraw-Hill, New York
3 Ali, M., Rellos, P. and Cox, T. (1998) Hereditary fructose intolerance. J. Med. Genet. **35**, 353–365
4 Santamaria, R., Scarano, M. I., Esposito, G., Chiandetti, L., Izzo, P. and Salvatore, F. (1993) The molecular basis of hereditary fructose intolerance in Italian children. Eur. J. Clin. Chem. Clin. Biochem. **31**, 675–678
5 Santamaria, R., Tamasi, S., Del Piano, G., Sebastio, G., Andria, G., Borrone, C., Faldella, G., Izzo, P. and Salvatore, F. (1996) Molecular basis of hereditary fructose intolerance in Italy: identification of two novel mutations in the aldolase B gene. J. Med. Genet. **33**, 786–788
6 Santamaria, R., Vitagliano, L., Tamasi, S., Izzo, P., Zancan, L., Zagari, A. and Salvatore, F. (1999) Novel six-nucleotide deletion in the hepatic fructose-1,6-bisphosphate aldolase gene in a patient with hereditary fructose intolerance and enzyme structure–function implications. Eur. J. Hum. Genet. **7**, 409–414
7 Santamaria, R., Esposito, G., Vitagliano, L., Race, V., Paglionico, I., Zancan, L., Zagari, A. and Salvatore, F. (2000) Functional and molecular modelling studies of two hereditary fructose intolerance-causing mutations at arginine 303 in human liver aldolase. Biochem. J. **350**, 823–828
8 Beutler, E., Scott, S., Bishop, A., Margolis, N., Matsumoto, F. and Kuhl, W. (1973) Red cell aldolase deficiency and hemolytic anemia: a new syndrome. Trans. Assoc. Am. Phys. **86**, 154–166
9 Miwa, S., Fujii, H., Tani, K., Takahashi, K., Takegawa, S., Fujinami, N., Sakurai, M., Kubo, M., Tanimoto, Y., Kato, T. and Matsumoto, N. (1981) Two cases of red cell aldolase deficiency associated with hereditary hemolytic anemia in a Japanese family. Am. J. Hemat. **11**, 425–437
10 Kishi, H., Mukai, T., Hirono, A., Fujii, H., Miwa, S. and Hori, K. (1987) Human aldolase A deficiency associated with a hemolytic anemia: thermolabile aldolase due to a single base mutation. Proc. Nat. Acad. Sci. U.S.A. **84**, 8623–8627
11 Kreuder, J., Borkhardt, A., Repp, R., Pekrun, A., Gottsche, B., Gottschalk, U., Reichmann, H., Schachenmayr, W., Schlegel, K. and Lampert, F. (1996) Brief report: inherited metabolic myopathy and hemolysis due to a mutation in aldolase A. New Eng. J. Med. **334**, 1100–1104
12 Hurst, J. A., Baraitser, M. and Winter, R. M. (1987) A syndrome of mental retardation, short stature, hemolytic anemia, delayed puberty, and abnormal facial appearance: similarities to a report of aldolase A deficiency. Am. J. Med. Genet. **28**, 965–970
13 Parano, E., Trifiletti, R. R., Barone, R., Pavone, P. and Pavone, V. (2000) Arthrogryposis multiplex congenita and pituitary ectopia: A case report. Neuropediatrics **31**, 325–327
14 Miller, S. A., Dykes, D. D. and Polesky, H. F. (1988) A simple salting out procedure for extracting DNA from human nucleated cells. Nucleic Acids Res. **16**, 1215
15 Newton, C. R., Graham, A., Heptinstall, L. E., Powell, S. J., Summers, C., Kalsheker, N., Smith, J. C. and Markham, A. F. (1989) Analysis of any point mutation in DNA. The amplification refractory mutation system (ARMS). Nucleic Acids Res. **17**, 2503–2516
16 Izzo, P., Costanzo, P., Lupo, A., Rippa, E., Paolella, G. and Salvatore, F. (1988) Human aldolase A gene: structural organization and tissue-specific expression by multiple promoters and alternate mRNA processing. Eur. J. Biochem. **174**, 569–578
17 Esposito, G., Vitagliano, L., Santamaria, R., Viola, A., Zagari, A. and Salvatore, F. (2002) Structural and functional analysis of aldolase B mutants related to hereditary fructose intolerance. FEBS Lett. **531**, 152–156
18 Morris, A. J. and Tolan, D. R. (1993) Site-directed mutagenesis identifies aspartate 33 as a previously unidentified critical residue in the catalytic mechanism of rabbit aldolase A. J. Biol. Chem. **268**, 1095–1110
19 Berman, H. M., Bhat, T. N., Bourne, P. E., Feng, Z., Gilliland, G., Weissig, H. and Westbrook, J. (2000) The Protein Data Bank and the challenge of structural genomics. Nat. Struct. Biol. **7**, 957–959
20 Gamblin, S. J., Davies, G. J., Grimes, J. M., Jackson, R. M., Littlechild, J. A. and Watson, H. C. (1991) Activity and specificity of human aldolases. J. Mol. Biol. **219**, 573–576
21 Blom, N. and Sygusch, J. (1997) Product binding and role of the C-terminal region in class I D-fructose 1,6-bisphosphate aldolase. Nat. Struct. Biol. **4**, 36–39
22 Dalby, A., Dauter, Z. and Littlechild, J. A. (1999) Crystal structure of human muscle aldolase complexed with fructose 1,6-bisphosphate: mechanistic implications. Protein Sci. **8**, 291–297
23 Choi, K. H., Mazurkie, A. S., Morris, A. J., Utheza, D., Tolan, D. R. and Allen, K. N. (1999) Structure of a fructose-1,6-bis(phosphate) aldolase liganded to its natural substrate in a cleavage-defective mutant at 2.3 Å. Biochemistry **38**, 12655–12664
24 Choi, K. H., Shi, J., Hopkins, C. E., Tolan, D. R. and Allen, K. N. (2001) Snapshots of catalysis: the structure of fructose-1,6-(bis)phosphate aldolase covalently bound to the substrate dihydroxyacetone phosphate. Biochemistry **40**, 13868–13875
25 Maurady, A., Zdanov, A., De Moissac, D., Beaudry, D. and Sygusch, J. (2002) A conserved glutamate residue exhibits multifunctional catalytic roles in D-fructose-1,6-bisphosphate aldolases. J. Biol. Chem. **277**, 9474–9483
26 Hutchinson, E. G. and Thornton, J. M. (1996) PROMOTIF – a program to identify and analyse structural motifs in proteins. Protein Sci. **5**, 212–220
27 Jones, T. A. and Kjeldgaard, M. (1997) Electron-density map interpretation. Methods Enzymol. **277**, 173–208
28 Laskowski, R. A., MacArthur, M. W., Moss, D. S. and Thornton, J. M. (1993) PROCHECK: a program to check the stereochemical quality of protein structures. J. Appl. Crystallogr. **26**, 283–291
29 Kraulis, P. J. (1991) MolScript: a program to produce both detailed and schematic plots of protein structures. J. Appl. Crystallogr. **24**, 945–949
30 Merritt, E. A. and Bacon, D. J. (1997) Raster3D: photorealistic molecular graphics. Methods Enzymol. **277**, 505–524
31 Minakami, S. Y. and Oshikawa, H. (1965) Thermodynamic considerations on erythrocyte glycolysis. Biochem. Biophys. Res. Commun. **18**, 345–349

Received 16 December 2003/4 February 2004; accepted 6 February 2004
Published as BJ Immediate Publication 6 February 2004, DOI 10.1042/BJ20031941